Use of Fabry-Pérot lasers for simultaneous distributed strain and temperature sensing based on hybrid Raman and Brillouin scattering

Marcelo A. Soto, Gabriele Bolognini and Fabrizio Di Pasquale
Scuola Superiore Sant'Anna, via G. Moruzzi 1, 56124 Pisa, Italy.
E-mail: g.bolognini@sssup.it

ABSTRACT

In this paper we propose the use of multi-longitudinal mode lasers, such as Fabry-Pérot (FP) lasers, for simultaneous distributed strain and temperature sensing based on hybrid Brillouin and Raman scattering. Fabry-Pérot lasers allow for high-power Raman intensity measurement and the simultaneous detection of the Brillouin frequency shift parameter for all FP longitudinal modes, by using a self-heterodyne detection scheme based on a multi-wavelength optical local oscillator. Experiments point out significant improvement in hybrid sensor performance, also suggesting further potential benefits when combining the use of FP lasers with optical coding techniques and/or optical amplification.

Keywords: Raman scattering, Brillouin scattering, fiber optic sensors, temperature sensing, strain sensing.

1. INTRODUCTION

Distributed temperature and strain fiber-optic sensors find significant applications in many areas, from structural-health monitoring of large structures, such as dams and bridges, to leakage and strain detection in power cables and pipelines, from early warning of landslides to borehole and underground mine monitoring. Most distributed strain and temperature sensors are currently based on Brillouin scattering measurements only [1] or on hybrid Raman-Brillouin scattering detection [2], in conjunction with optical time domain reflectometry (OTDR) techniques. In systems based on spontaneous Brillouin scattering (SpBS), the simultaneous detection of both spontaneous Brillouin intensity and Brillouin frequency shift (BFS) allows one to distinguish strain and temperature changes into the same sensing fiber. This scheme requires access to one fiber-end only but its performance is seriously affected by the low backscattered power values. Also stimulated Brillouin scattering (SBS) effect can be exploited to measure the BFS, providing better resolution, but requiring access to both fiber ends; in such schemes the strain-temperature cross sensitivity issue is often overcome by using two sensing fibers, only one of them embedded in the structure to be monitored. On the other hand, in hybrid Raman-Brillouin schemes [2], the temperature profile along the sensing fiber is directly obtained by measuring the spontaneous anti-Stokes Raman signal, which is strain independent. Thus, the temperature profile is then used to estimate the strain along the fiber derived from the BFS measurement, which is both temperature and strain dependent. The main issues affecting hybrid sensors performance are mainly related to the different Brillouin and Raman scattering cross-sections, leading to significantly different backscattered power levels. Hence, the resulting noise in spontaneous Raman scattering (SpRS) measurement is actually the main limiting factor in temperature-strain measurements with hybrid sensing [2]. In order to overcome this limitation, higher input pump power levels should be used, limiting however the maximum usable power below the onset on nonlinear effects [3], such as stimulated Raman and Brillouin scattering, having different characteristics in both cases. Furthermore, the optical sources commonly used for SpBS measurements are characterized by rather low output power levels; actually, in order to comply with the narrow Brillouin gain bandwidth (few tens of MHz in silica fibers), narrowband optical sources, such as distributed feedback lasers (DFB) or external cavity lasers (ECL), are used [2], with a typical output power below few tens of mW. Hence, the requirements imposed by the Brillouin measurement do not seem to be compatible with the need of high power and broad bandwidth sources which can be effective for the Raman measurement. A smart usage of optical sources available on the market, to overcome the limitations imposed by both narrowband Brillouin gain and low-level Raman scattering light could be of great benefit when implementing highly-accurate distributed strain and temperature sensors.

In this work we propose the use of multi-longitudinal mode Fabry-Pérot (FP) lasers for simultaneous distributed strain and temperature sensing based on hybrid Raman-Brillouin measurements. To improve the sensing performance, a novel detection scheme based on a multi-wavelength optical local oscillator (OLO) is also proposed, allowing for the simultaneous measurement of the BFS for all FP modes by using a single photodetector and a coherent detection scheme. We show that the use of FP lasers provide significant accuracy improvement in both temperature and strain sensing.

20th International Conference on Optical Fibre Sensors, edited by Julian Jones, Brian Culshaw, Wolfgang Ecke, José Miguel López-Higuera, Reinhardt Willsch, Proc. of SPIE Vol. 7503, 750328
© 2009 SPIE · CCC code: 0277-786X/09/$18 · doi: 10.1117/12.834952

Downloaded From: http://spiedigitallibrary.org/ on 11/01/2012 Terms of Use: http://spiedl.org/terms

2. THEORY

In hybrid Raman-Brillouin sensors for strain and temperature measurement, both SpRS and SpBS lights are simultaneously detected. The temperature dependence of the anti-Stokes SpRS signal allows for a strain-independent measurement, so that, the temperature profile along the sensing fiber is directly obtained by using the ratio of the anti-Stokes Raman power (P_{AS}) over the Rayleigh-backscattering power (P_{BS}), which is dependent on the absolute temperature according to:

$$\frac{P_{AS}}{P_{BS}} \propto \left[\exp\left(\frac{h\Delta\nu_R}{kT}\right)-1\right]^{-1} \quad (1)$$

where h is the Planck constant, k is the Boltzmann constant, T is the absolute temperature, and $\Delta\nu_R$ is the separation between anti-Stokes Raman and pump light frequencies. Changes in the distributed strain ($\Delta\varepsilon$) along the fiber can be estimated from the BFS measurement ($\Delta\nu_B$), which linearly depends on both strain and temperature according to:

$$\Delta\nu_B = C_{\nu_B\varepsilon}\cdot\Delta\varepsilon + C_{\nu_B T}\cdot\Delta T \quad (2)$$

where $C_{\nu B\varepsilon}$ = 0.048 MHz/με and $C_{\nu BT}$ = 1.07 MHz/°C are the strain and temperature coefficients for Brillouin frequency shift [1]. Thus, the temperature variation in Eq. (2) is provided by Eq. (1) based on anti-Stokes Raman measurement, allowing for a temperature-independent strain estimation.

Fabry-Pérot semiconductor lasers are inherent multi-wavelength optical sources, with a grid of narrowband longitudinal modes exhibiting a frequency difference depending on the laser-cavity length, typically of the order of tens of GHz (lasers with typical laser cavity lengths of hundreds of micrometers). Due to their high power levels (commonly operating around few hundreds of mW), high-power FP lasers can be fruitfully exploited in Raman sensors, enabling accurate measurements. They also possess the advantage of having a large full width half maximum (FWHM, typically several nm), allowing for Rayleigh measurements which are not affected by coherent-Rayleigh noise (CRN) [4].

Note that, when a FP laser is used for Raman sensing measurements, each longitudinal mode also generates SpBS. The FWHM of *each* FP mode is generally narrower than the Brillouin gain bandwidth, and also the spectral separation among adjacent modes is typically larger than twice the BFS in silica. These features allow one to clearly identify the Stokes and anti-Stokes Brillouin components for each longitudinal mode of the FP laser. Our goal is then to exploit the SpBS generated by *all* FP modes in order to obtain the BFS parameter. Note that hybrid Raman-Brillouin sensing based on single longitudinal mode lasers, e.g. DFB lasers [2], has the limitation of Raman-temperature inaccuracy due to the low-power level of the lasers. Thus, by exploiting the high-power features of FP lasers we can overcome this limitation, providing a notably better performance. As an additional point, while the anti-Stokes Raman intensity is measured by a simple direct-detection scheme, BFS measurement requires instead a coherent-detection receiver [1]. In such schemes, the SpBS signal is amplified when mixing with an OLO, offering higher dynamic range compared to direct-detection and, the conversion of the optical Brillouin components to the electric domain, leading to efficient electric spectral filtering [1]. Finally, we have recently demonstrated that optical pulse coding techniques provide an enhanced SNR in SpBS-based sensors [5], allowing for an improved sensing performance. However, the use of coding is limited by the SBS threshold, which constraints the maximum optical power at the fiber input [5]. In our proposed scheme employing FP lasers this limitation can be overcome because the total laser power is distributed among several longitudinal modes, each one being limited by the SBS threshold, thus allowing for higher total peak power levels. Due to the reduced peak power of every FP mode, the proposed technique can also be used in conjunction with optical pulse coding as well as with optical amplification (to further increase laser power) for achieving additional sensing performance improvement.

3. EXPERIMENTAL SET-UP

The used set-up is reported in Fig. 1; two different kinds of lasers, namely DFB laser and FP laser, are alternatively used in order to compare their performances for hybrid Raman-Brillouin sensing. The maximum output power of the used DFB lasers is P_{DFB} = 8.5 dBm at 1550 nm, allowing us to attain P_{IN} = 1.5 dBm at fiber input. Current dithering is also required for the DFB laser when measuring the Rayleigh backscattered light (which is necessary to obtain loss-independent measurements) in order to reduce CRN. On the other hand, FP lasers typically attain higher power levels (ranging from 20-26 dBm); in our experiments the power was P_{FPL} = 22 dBm at the FP laser output, allowing for P_{IN} = 15 dBm at fiber input. As a further benefit, the total linewidth of the FP laser is large enough, thanks to the multiple longitudinal modes, so that CRN in Rayleigh measurements is inherently reduced due to wavelength averaging. The CW-light of the source is split into two parts using a 10/90 optical coupler, so that 10% of the light is used at the receiver-side as OLO and the other 90% is modulated (at the transmitter-side) with 350 ns single pulses allowing for 35 m spatial resolution. Optical

Downloaded From: http://spiedigitallibrary.org/ on 11/01/2012 Terms of Use: http://spiedl.org/terms

pulses are launched into 25 km of standard single mode fiber (SSMF), and the backscattered light is then coupled into the receiver-side, which is composed of three stages. The first stage (Raman receiver) consists in a WDM filter separating the light band around 1450 nm from the band around 1550 nm, so that the anti-Stokes SpRS component can be separated and coupled into an avalanche photodiode (APD) followed by a trans-impedance amplifier (TIA) and an analog-digital converter (ADC) connected to a computer (PC). The second stage (Rayleigh receiver), consisting in a direct-detection receiver, is used for Rayleigh-scattering measurements and is composed of a PIN photodiode, a TIA and an ADC connected to the PC. The third stage (Brillouin receiver) consists in an optical and electrical heterodyne receiver, including an electrical spectrum analyzer (ESA), operating in zero-span mode. A polarization scrambler (PS) has been used to reduce polarization-induced fading noise, reducing the degree of polarization of the FP laser down to ~ 1%.

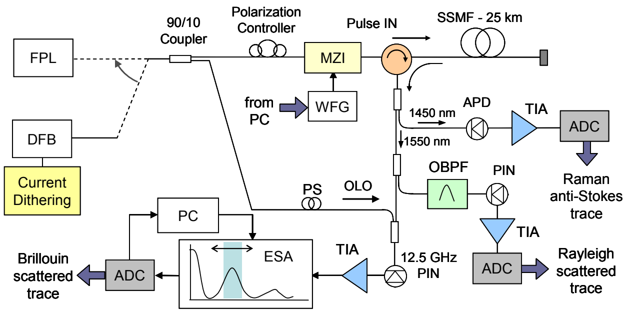

Fig. 1. Experimental set-up of hybrid Raman-Brillouin distributed strain and temperature sensor

Note that, since the lightwave spectrum of a FP laser consists of a comb of equally frequency-spaced longitudinal modes, each mode (after propagation along the fiber) generates a couple of Stokes and anti-Stokes SpBS lines, as shown Fig. 2a. In order to simultaneously measure the BFS parameter for all FP longitudinal modes with a single photodetector, we require the use of a multi-wavelength OLO. The set-up shown in Fig. 1 actually allows the proposed self-heterodyne detection scheme, so that Brillouin components are heterodyned with the multi-wavelength OLO, obtained by splitting a portion of the same FP laser. Fig. 2a reports a zoom of the spectrum (with normalized peak power) of five modes of the used FP laser and the respective Rayleigh, Stokes and anti-Stokes SpBS components. The spectral separation between two consecutive modes is 0.3 nm, corresponding to more than twice the BFS and allowing for BFS separation among different modes. This condition actually needs to be satisfied in order to avoid possible overlapping of Stokes and anti-Stokes components of two neighbouring modes. Also, the peak mode power of the OLO needs to be much higher than the peak power of every Rayleigh backscattered mode in order to avoid distortions in the heterodyning process due to beating of Rayleigh and SpBS signals. Thus, when heterodyning the multi-wavelength OLO with the backscattered light from the fiber, only a single beating signal is produced at around 10.94 GHz, as shown Fig. 2b. This signal lies within the Brillouin gain bandwidth, and represents the summed contribution of Stokes and anti-Stokes components generated by all FP modes, allowing the simultaneous detection of the average SpBS spectrum (and then the average BFS) with a single photodetector, and leading to an improved SNR with respect to the detection of a single longitudinal mode. Then, the measured spectrum is fitted with a Lorentzian curve at each fiber position, so that the average BFS is obtained. The fitted spectrum versus fiber distance is reported in Fig. 2b, also showing the data fitting at 5 km distance (Fig. 2b inset).

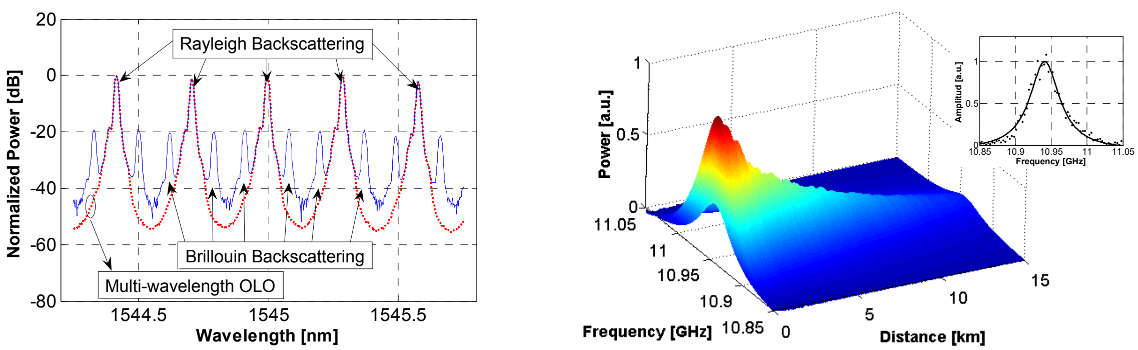

Fig. 2. (a) Spectrum of the used FP laser and respective Rayleigh, Brillouin Stokes and anti-Stokes components. (b) Brillouin signal in electrical domain (~ 10.9 GHz) representing the summed contribution of all FP modes. Inset. Lorentzian fitting to measured spectrum at 5km distance.

4. RESULTS

To measure the Brillouin spectrum profile as a function of the distance, the coherent self-heterodyne detector of Fig. 1 has been used. The FP laser employed in the experiment has about 30 longitudinal modes (~7 dBm power per mode), each one able to generate a couple of Stokes and anti-Stokes SpBS components. The same laser is also used as a multi-wavelength OLO, which is mixed at the PIN photodiode together with the SpBS components, scattered from the sensing fiber (both signals are shown in Fig. 2a, with normalized peak power).

Downloaded From: http://spiedigitallibrary.org/ on 11/01/2012 Terms of Use: http://spiedl.org/terms

Although the use of multi-wavelength optical sources allows in principle for a higher optical backscattered power, the experimental *rms* error in the average BFS, obtained by using the FP laser, is higher than the obtained with the DFB laser, as shown Fig. 3 (in this case, every trace has been averaged 150k times). This result indicates the occurrence, when employing FP lasers, of some noise issues that can be related to optical phenomena such as the wavelength-dependence in BFS or the frequency drift of the FP modes. However, as clearly visible in Fig. 4, the increased noise in BFS has only a small impact on the ultimate strain-temperature resolution, since the limiting factor in hybrid sensing is essentially given by the noise in anti-Stokes Raman intensity measurement [2], where the use of the FP laser has a strong beneficial impact.

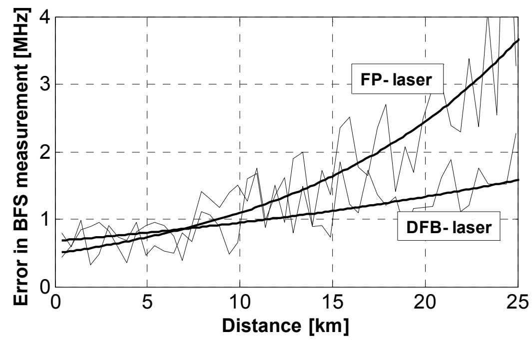

Fig. 3. Error in BFS measurement vs distance, for both DFB and FP lasers.

A high accuracy in intensity measurements has actually been achieved when using the FP laser. The achieved temperature resolution δT is shown in Fig. 4a, indicating that a value of δT~20 K (at 25 km distance) obtained with a DFB laser can be improved down to δT~1.2 K by using the FP laser (attaining $\delta T < 0.2$ K within the first 10 km of fiber). Note that in sensor performance analysis, it is not required to apply any actual strain or temperature change to the fiber, since attainable resolution parameters depend ultimately on the SNR of the measured traces. When calculating the final *temperature-independent* strain distribution (and hence the strain resolution), the accuracy enhancement in anti-Stokes Raman intensity has a significant impact. Fig. 4b actually indicates that a strain resolution of ~470 με at 25 km distance, obtained with the DFB laser, can be improved down to ~100 με when using the FP laser.

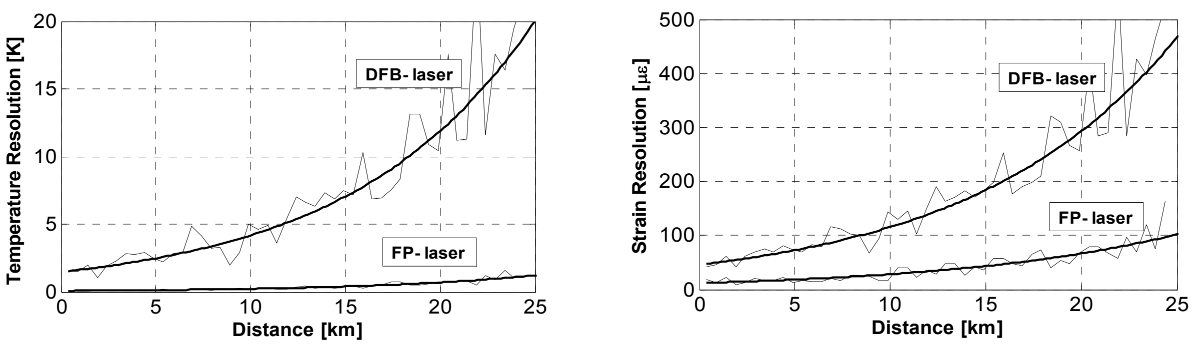

Fig. 4. (a) Temperature resolution and (b) strain resolution vs distance, for both DFB and FP lasers.

5. CONCLUSIONS

In conclusion we have proposed the use of multi-wavelength FP lasers for simultaneous strain and temperature measurements based on hybrid Brillouin-Raman distributed optical sensors, allowing for a significant sensing performance improvement. The multiple longitudinal modes of FP lasers provide a power distribution along the spectrum, overcoming the limitation of the maximum peak pulse power at the fiber input, imposed by nonlinearities, such as SBS threshold, allowing for further improvement when using optical pulse techniques or optical amplification.

REFERENCES

[1] S. M. Maughan *et al.*, "Simultaneous distributed fibre temperature and strain sensor using microwave coherent detection of spontaneous Brillouin backscatter," *Meas. Sci. Technol.*, vol 12, pp. 834-842, 2001.
[2] M. N. Alahbabi *et al.*, "Simultaneous temperature and strain measurement with combined spontaneous Raman and Brillouin scattering," *Opt. Lett.*, vol. 30, no. 11, pp. 1276-1278, 2005.
[3] P. C. Wait *et al.*, "A theoretical comparison of spontaneous Raman and Brillouin based fibre optic distributed temperature sensors," *Opt. Commun.* 144, pp. 17-23, 1997.
[4] K. De Souza, "Significance of coherent Rayleigh noise in fibre-optic distributed temperature sensing based on spontaneous Brillouin scattering," *Meas. Sci. Technol.*, vol. 17, pp. 1065-1069, 2006.
[5] M. A. Soto *et al.*, "Analysis of optical pulse coding in spontaneous Brillouin-based distributed temperature sensors," *Opt. Express*, vol. 16, n. 23, pp 19097-19111, 2008.

Downloaded From: http://spiedigitallibrary.org/ on 11/01/2012 Terms of Use: http://spiedl.org/terms